Development and characterization of Protein Kinase B/AKT isoform-specific Nanobodies

Tijs Merckaert
Universiteit Gent https://orcid.org/0000-0002-8185-4766
Olivier Zwaenepoel
Universiteit Gent
Kris Gevaert
Universiteit Gent
Jan Gettemans (Jan.gettemans@ugent.be)
https://orcid.org/0000-0001-6979-8872

Research

Keywords: nanobodies, VHH, single-domain-antibody, intrabody, Protein Kinase B, AKT, cancer

Posted Date: March 26th, 2020

DOI: https://doi.org/10.21203/rs.3.rs-18280/v1

Version of Record: A version of this preprint was published at PLOS ONE on October 12th, 2020. See the published version at https://doi.org/10.1371/journal.pone.0240554.

Abstract

Background The serine/threonine protein kinase AKT is frequently over-activated in cancer and is associated with poor prognosis. As a central node in the PI3K/AKT/mTOR pathway, which regulates various processes considered to be hallmarks of cancer, this kinase has become a prime target for cancer therapy. However, AKT has proven to be a highly complex target as it comes in three isoforms (AKT1, AKT2 and AKT3) which are highly homologous, yet non-redundant. The isoform-specific functions of the AKT kinases can be dependent on context (i.e. different types of cancer) and even opposed to one another. To date, there is no isoform-specific inhibitor available and no alternative to genetic approaches to study the function of a single AKT isoform.

Results We have developed and characterized nanobodies that specifically interact with the AKT1 or AKT2 isoforms. These new tools should enable future studies of AKT1 and AKT2 isoform-specific functions. Furthermore, for both isoforms we obtained a nanobody that interferes with the AKT-PIP3-interaction, an essential step in the activation of the kinase.

Conclusions The nanobodies characterized in this study, which can be expressed in mammalian cells, are a new stepping stone towards unravelling AKT isoform-specific signalling and can lead to the first isoform-specific AKT inhibitor.

Background

The PI3K/AKT/mTOR pathway is one of the most frequently dysregulated pathways in cancer, with up to 30% of human cancers displaying mutations in one or several members of this pathway(1, 2). One of its central nodes, the Ser/Thr protein kinase AKT (also known as Protein Kinase B), regulates multiple cellular processes, among them cell survival, metabolism, growth and proliferation(1). Although AKT itself is rarely mutated, the proteins that regulate AKT such as PI3K, PTEN and PHLPP are frequently mutated, resulting in increased AKT activity, tumour cell growth and survival(3). This made AKT an attractive target for the treatment of tumours with PI3K/AKT/mTOR pathway mutations(4, 5). However, the development of small-molecule AKT inhibitors has long been hampered by the structural similarity of the AKT catalytic domain to that of other kinases of the AGC kinase group(5–7). In addition, there are several known cases of ATP-competitive inhibitors that induce AKT hyperphosphorylation and activity(8). To overcome such issues, the focus shifted towards the development of allosteric inhibitors (such as MK-2206, miransertib and AKT1/2), which show highly improved specificity towards AKT(5, 9, 10). In recent years however, it has become clear that specificity for the AKT family is not sufficient (11). The AKT kinase comes in three isoforms (AKT1, AKT2 and AKT3) each encoded by a separate gene(12). All AKT isoforms share the same basic building blocks: an N-terminal Pleckstrin homology (PH) domain, a linker, catalytic domain and C-terminal regulatory domain(12). In unstimulated cells the PH-domain keeps AKT in an inactive conformation (PH-in) through interaction with the catalytic domain. In response to upstream signalling – the interaction of the PH-domain with phosphatidylinositol (3,4,5)-trisphosphate (PIP3) produced by PI3K – AKT shifts to an open conformation (PH-out) enabling activation by

phosphorylation on a threonine residue in the catalytic domain and a serine residue in the C-terminal regulatory domain(5, 13–15). The isoforms are highly homologous with 82% sequence identity for AKT1 vs AKT2, 83% for AKT1 vs AKT3 and 77% for AKT2 vs AKT3. Despite their homology, they have non-redundant and, in certain cases, opposed functions (11, 16–24). A striking example are the roles of AKT1 and AKT2 in breast cancer where AKT2 enhances migration and invasion, whereas AKT1 inhibits these processes(16, 19, 20, 25, 26). This underlines the need for new tools to study AKT isoform-specific functions, which directly affect the protein, rather than the proteins' expression levels. Such tools can also be a first step towards the development of a specific inhibitor. Indeed, targeting a single AKT isoform to counteract the function of the drivers relevant to a specific type of cancer would alleviate the toxicity observed when using pan-AKT inhibitors and be beneficial for patient outcome(27).

The serum of alpacas and other members of the camelidae family contain Heavy-Chain-Only antibodies (HCAb). This subtype of IgG, discovered by the Hamers-Casterman group, completely lacks light chains (LC) and the first constant domain of the heavy chain (HC)(28). The antigen-binding fragment of such a HCAb consists of a single domain that remains functional when isolated. This domain, called a variable domain of the heavy chain of a HCAb (VHH) or a nanobody (Nb), is approximately 15 kDa in size and measures 2.5 by 4 nm(29, 30). Structurally, a Nb is composed of four well conserved framework regions (FR) and three hypervariable regions (HV), the latter forming loops that cluster at the N-terminal side of the folded Nb, where they form the antigen-binding surface or complementarity-determining region (CDR). The HV loops of a Nb are usually longer than those found in the variable domain of the heavy chain (VH), to compensate for the lack of the variable domain of the light chain (VL) which, in conventional Abs, forms the CDR together with the VH. The three HV loops of the Nb provide a CDR of 600–800 Å which, unlike the CDR of a conventional Ab, forms a convex surface(29–32). In conventional Abs, the main chain atoms of the variable loops can only adopt a few different conformations, called canonical structures. However, the HV loops of a Nb are not limited to such canonical conformations (32) and therefore, Nbs can bind clefts on protein surfaces which cannot be targeted by conventional Abs(33). As such, Nbs are small, stable, single-domain and high-affinity binders that can access cryptic epitopes(29).

To date there are no alternatives to genetic manipulation to study/interfere with the function of a single AKT isoform. The allosteric inhibitors, currently the most promising candidates for therapeutic AKT inhibition, function by binding the PH domain and locking AKT in the PH-in conformation, thereby preventing AKT activation(5, 10). To obtain isoform-specific AKT nanobodies that interact with the AKT PH-domains, an alpaca was immunized with recombinant AKT1 PH-domain (AKT1PH) or the mutant form which confers constitutive membrane localization and activation of AKT1 (AKT1PHE17K), full-length and activated AKT2 (AKT2FL) or the AKT3 PH-domain (AKT3PH)(13). Using this approach, we obtained AKT1 and AKT2-specific binders, which can be expressed as intrabodies in mammalian cells. Furthermore, both for AKT1 and AKT2, a single specific Nb was obtained that interacts with the PH-domain and interferes with the AKT-PIP3-interaction in vitro. As AKT isoform-specific interactors, these Nbs offer new possibilities to study and interfere with the functions of these kinases at the protein level. As such, these new tools can be a step towards solving the complex roles of the AKT isoforms.

Results

Generation of AKT Nanobodies

The AKT1-, AKT1PHE17K- and AKT3-PH domains were expressed in BL21 E. coli cells, purified using TALON®-immobilized metal affinity chromatography (IMAC) (Clontech) and subsequent anion-exchange chromatography (MonoQ, GE Healthcare). Purity of the eluted fractions was assessed by SDS-PAGE. Purified and active AKT2 was purchased from Active Motif (Additional file 1: Figure S1).

Three separate VHH libraries were constructed: one for AKT1PH, the second for AKT1PHE17K and AKT3PH, and the third for AKT2FL. The libraries for AKT1PH and AKT2FL were constructed using the pMECS phagemid vector and contained 5×10^7 independent transformants (~ 87% with correct insert size) and 3×10^8 independent transformants (~ 80% with correct insert size) respectively. For AKT1PHE17K and AKT3PH, the pHEN4 phagemid vector was used and a library with 7.7×10^7 independent transformants (~ 93% with correct insert size) was obtained. Panning (2 rounds for AKT1PH and 4 rounds for AKT1PHE17K, AKT3PH and AKT2FL), enzyme-linked immunosorbent assay (ELISA) on crude periplasmatic extracts and sequencing of positive colonies yielded 17 AKT1PH Nbs, 8 AKT1PHE17K Nbs, 10 AKT2FL Nbs and 11 AKT3PH Nbs.

Screening for AKT isoform-specific binders

Nb expression was assessed though Western blot analysis of WK6 E. coli crude periplasmatic extracts (Fig. 1). Almost all Nbs were successfully expressed at high levels, AKT1PH Nb14 and Nb15, AKT1PHE17K Nbs5-8, AKT2FL Nb10 and AKT3PH Nb1 were expressed at lower levels. Only AKT1PHNb17 and AKT3PHNb11 did not yield any signal indicating extremely low, or no, expression. The AKT PH-domain Nb sets (AKT1PH-, AKT1PHE17K- and AKT3PHNbs) were screened for strength of interaction and specificity through ELISA (Fig. 2). In contrast to the ELISA performed during panning, where each library was screened for interaction with its corresponding PH-domain, each Nb was tested for cross-reactivity with each of the available AKT PH-domains (AKT1PH, AKT1PHE17K, AKT2PH and AKT3PH). A Nb is considered to interact with a PH-domain when the measured optical density $(OD)_{405}$ is at least three times higher than that of the EGFP Nb (negative control) for the corresponding PH-domain (OD fold change > 3, denoted as dashed line in Fig. 2). In this manner, Nbs were excluded from further characterisation due to low binding. 8 AKT1PH Nbs met the OD requirement. AKT1PH domain Nbs1-5, Nb8 and Nb10 all have similar interaction profiles with no clear preference for interacting with the AKT1PH domain over the mutant form (AKT1PHE17K) or the PH-domains from AKT2 and AKT3. AKT1PH Nb16 also interacts with all 4 PH domain constructs, but shows some preference towards AKT1 and AKT1PHE17K as the OD fold change is significantly higher ($p < 0.001$) for these PH-domains. AKT1PHE17K Nb7 (refered to as M.7 in the figure legend) interacts with both AKT1PH and AKT1PHE17K, but shows no true preference for interacting with the mutant form (AKT1PHE17K) of this PH-domain ($p > 0.05$). AKT3PH Nb7, one of three Nbs from the AKT3PH set with OD fold change > 3 interacts withAKT1PH, AKT1PHE17K and AKT3PH. Judging by the OD fold change, this Nb binds more strongly

with both the wild type and mutant form of the AKT1 PH domain than with the AKT3PH domain ($p < 0.05$). AKT3PH Nb8 and Nb9 both interact with AKT3PH but hardly with the PH-domains of the other AKT isoforms. It should be noted that, for AKT3PH Nb8, the measured OD_{405} for the other PH-domains almost reached the OD fold change requirement for being considered an interactor. This initial screening was performed to select for Nbs that have the greatest potential to be isoform-specific binders. The ELISA for the AKT1PH-, AKT1PHE17K- and AKT3PH-domain Nbs indicated that we have obtained a single Nb specific for AKT1 (which binds both wild type and the E17K mutant) and two AKT3-specific Nbs. Additionally, AKT1PH Nb8 was included in further screening experiments as pan-AKT Nb and AKT3PH Nb7 as an AKT1 & AKT3 interactor.

Interaction of these Nbs with endogenous full-length AKT1, AKT2 and AKT3 isoforms from MDA-MB-231 cells was determined through Co-Immunoprecipitation (Co-IP) using recombinantly produced hemagluttin (HA)-tagged Nbs. As the AKT2FL Nbs were produced using full-length AKT2, the entire AKT2FL Nb set was included in this analysis. As shown by the clear band at ~ 15 kDa, all Nbs were efficiently produced in WK6 E. coli and enriched on the anti-HA-agarose beads (Fig. 3). As the ELISA screening indicated that the AKT1PH domain Nbs do not show specificity for a single isoform PH domain, a single representative Nb, AKT1PH Nb8, was selected. Western blot analysis (Fig. 3) of the Co-IP using AKT isoform-specific antibodies showed AKT1PH Nb8 to recognize endogenous AKT1 and AKT2, but not AKT3 (lane 1.8 in Fig. 3A, B and C). AKT1PHE17K Nb7, pulled-down only the AKT1 isoform (Fig. 3A lane 1M7). From the set of 10 AKT2FL Nbs, AKT2FLNb10, Nb9, Nb7, Nb5, Nb8 and Nb6 (arranged by decreasing AKT2 signal intensity) were able to pull-down AKT2 (Fig. 3B lanes 2.5–2.10). Although Nbs 1–4 were expressed to similar extent, no AKT2 was detected for these Nbs (Fig. 3B lanes 2.1–2.4). For determining cross-reactivity with AKT1 and AKT3, AKT2FL Nb2 was chosen and AKT2FL Nb1, Nb3 and Nb4 were omitted. For AKT2FL Nb2, no AKT1 or AKT3 could be detected, as such, AKT2FL Nbs1-4 excluded from further experiments. Of the 6 Nbs that were able to pull-down AKT2, both Nb7 and Nb10 cross-reacted with AKT1 (Fig. 3A lanes 2.7 and 2.10). Furthermore, Nb10 also interacts with AKT3 (Fig. 3C lane 2.10), but to a much lesser extent. AKT3PH Nb7 was able to pull-down both AKT1 and AKT3 (Fig. 3A and C lane 3.7). AKT3PH Nb8 and AKT3PH Nb9 pulled-down AKT3 to a similar extent however, both Nbs also interacted with the AKT1 and AKT2 isoforms (Fig. 3A, B and C lanes 3.8 and 3.9).

Taken together with the ELISA screening, these results indicate immunization with the AKT1 PH domain did not yield Nbs specific for this isoform. The AKT1PHE17K immunization yielded a single Nb (AKT1PHE17K Nb7) that interacted with both the wild-type and the mutant form of the AKT1 PH-domain in an ELISA experiment and only pulls-down AKT1 in a Co-IP experiment. For AKT2, we obtained a set of 4 Nbs (AKT2FL Nb5, Nb6, Nb8 and Nb9) that only interacted with AKT2 in a Co-IP and 2 Nbs (AKT2FL Nb7 and Nb10) that interacted with several isoforms. Due to the low signal for AKT2, Nb6 was excluded from further experiments. No AKT3-specific Nbs were obtained as AKT3PH Nb7 also interacted with AKT1 and AKT3FL Nb8 and Nb9 bind all three isoforms in Co-IP experiments.

Epitope Mapping of AKT2FL nanobodies.

To narrow down the AKT2 domain(s) bound by the AKT2FL Nbs, constructs were designed for recombinant expression of full-length AKT2 (FL-AKT2), the AKT2 PH-domain (AKT2PH), AKT2 lacking the PH-domain (AKT2AA111) and the C-terminal regulatory domain (AKT2REG) (Fig. 4A). Nb-protein interaction was determined by ELISA (Fig. 4B). All tested Nbs bind FL-AKT2 with a fold change in normalized OD of 6.66 ± 0.8, 18.9 ± 1.6, 18.1 ± 0.7 and 18.69 ± 1.7 for Nbs 5, 8, 9 and 10 respectively. This indicates that, even though the Nbs were produced by immunization with active (phosphorylated) AKT2, the Nbs can also bind unphosphorylated AKT2, this being AKT2 in its inactive conformation. Nb9 is the only Nb to interact with the AKT2 PH-domain (OD fold change 19.1 ± 0.6). Nbs 5, 8 and 10 interacted with AKT2AA111 (OD fold change of 4.02 ± 0.27, 21.18 ± 0.3 and 20.8 ± 0.4 respectively). Both Nb8 and Nb10 also interacted with the regulatory domain (OD fold change of respectively 19.3 ± 3.66 and 18.97 ± 3.74) whereas Nb5 did not, suggesting Nb5s' epitope to be located on the flexible linker, kinase domain or a region overlapping the boundary of the kinase- and regulatory domain.

It was previously shown that Nbs can be used as the primary antibody for detection of proteins through Western blotting(34). This depends on the type of epitope the Nb interacts with (linear vs. conformational). None of the AKT Nbs were able to detect AKT in crude lysates from MDA-MB-231 cells, indicating that the Nbs interact with a conformational epitope which is lost on denaturation of AKT during sample preparation.

AKT Pleckstrin Homology domain Nbs interfere with PIP3 interaction

Interaction of the AKT Pleckstrin Homology domains with PIP3 is responsible for the membrane recruitment of the AKT isoforms, where they can be activated(14). Nbs that interact with the PH-domain have the potential to interfere with this interaction, thereby inhibiting the activation of the AKT kinases. A protein pull-down experiment using agarose beads coated with PIP3, recombinantly produced AKT PH-domains and AKTPH Nbs showed AKT1PHE17K Nb7 and AKT2FL Nb9 to compete with the PIP3-PH-domain interaction for AKT1PH / AKT1PHE17K and AKT2PH respectively (Fig. 5, lanes M.7 and 2.9). A pre-incubation of PH-domain and Nb reduced the amount of PH-domain pulled down by the PIP3-coated beads as determined by Western blot detection of the AKT PH-domains. AKT3PH Nb8 had no effect on the PIP3-PH-domain interaction for any PH-domain.

Transient expression of AKT Nbs in mammalian cells

MDA-MB-231 cells were transfected for transient expression of the AKT Nbs and the EGFP Nb, which served as negative control throughout this experiment. Analysis of the crude lysate (Fig. 6B) indicated that not all Nbs were expressed to the same extent: the EGFP Nb (C) displays the highest expression levels closely followed by AKT2FL Nb5 (2.5). AKT2FL Nb8 (2.8) and AKT3PH Nb8 (3.8) clearly have lower expression levels (although the signal for the loading control for AKT3PH Nb8 is lower as well), while AKT1PHE17K Nb7 (M.7) and AKT2PH Nb9 (2.9) could not be detected in crude lysate. Results from the Co-IP (Fig. 6A) showed that AKT1PHE17K Nb7 expression is detectable when enriched by the anti-V5-agarose, while the AKT2FL Nb9 signal remains low under these conditions. The majority of the AKT Nbs

is unable to pull-down any AKT, only AKT3PH Nb8, which interacts with all three isoforms has a clear signal for AKT.

Discussion

Targeting the AKT PH-domain has shown to be a promising strategy for interfering with AKT function: allosteric inhibitors such as MK-2206 and miransertib show superior selectivity for AKT over related kinases when compared to ATP-competitive inhibitors(5, 10, 35). However, these inhibitors still target all AKT isoforms, which can be detrimental for cancer treatment considering the different and sometimes opposed functions of the AKT isoforms(4, 16). In this study, we report the generation and characterisation of nanobodies specific for a single AKT isoform that interact with the PH-domain. Nb sets were generated by immunization of alpacas with the PH-domain of AKT1, AKT1PHE17K (an oncogenic AKT1 mutant), the full-length and activated AKT2 and the AKT3PH-domain. The obtained Nb sets were screened for specificity for a single AKT isoform through ELISA using recombinantly produced antigen and Co-IP using endogenous full-length AKT isoforms in crude lysate from MDA-MB-231 cells.

Due to the high degree of sequence identity for the AKT PH-domains, most of the obtained Nbs did not specifically interact with a single AKT isoform. The AKT1PH Nbs interact with all four PH-domains. A single representative (AKT1PH Nb8) was included for the Co-IP where it pulled-down AKT1 and AKT2, but not AKT3. This deviation from the results observed in the ELISA could be explained by the much lower expression levels of AKT3 in MDA-MB-231 cells compared to AKT1 and AKT2 (unpublished results). The AKT3 PH-domain Nb set did not yield any isoform specific Nbs. Even though the ELISA screening suggested AKT3PH Nb9 to be AKT3-specific, Co-IP of the endogenous AKT isoforms did not corroborate this. It is possible that the particular epitope bound by these Nbs is no longer available when AKT1PH, AKT1PHE17K or AKT2PH-domains are coated on the multiwell plate. As the main goal of this study is to identify isoform-specific Nbs that interact with the PH-domain, the AKT1PH- and AKT3PH-domain Nbs were omitted from further experiments.

AKT1PHE17K Nb7 interacts with both the wild-type and mutant AKT1PH-domains. Co-IP on endogenous AKT confirmed the AKT1-specificity. This indicates that binding of this Nb to the AKT1PH domain is not influenced by the conformational changes induced by the E17K mutation whereas this is known to confer resistance to the PH-domain targeting allosteric inhibitor Akti-1/2 and, although not linked to higher AKT1 activity, a decreased effect of MK-2206 on the phosphorylation of AKT1 S473(36–38). The AKT2FL Nb set contained 6 Nbs that were able to pull-down AKT2 from MDA-MB-231 cells, only 4 of those (Nbs 5, 6, 8 and 9) were specific for AKT2. Nb6 was excluded due to low signal. This set yielded a single Nb that interacts with the AKT2 PH-domain (Nb9), one that interacts with the regulatory domain (Nb8) and one binds the linker or kinase domain (Nb5).

Both AKT1PHE17K Nb7 and AKT2FL Nb9 could, for their respective AKT isoforms, interfere with the interaction between the recombinant PH-domain and PIP3-coated beads in an in vitro assay. For AKT1PHE17K Nb7 this includes both the wild-type PH-domain and the oncogenic mutant. These Nbs,

when expressed as intrabodies in cells, can potentially interfere with the activation of AKT1 or AKT2: AKT bound by one of these Nbs would be stuck in an inactive ‘PH-in’ conformation(15).

However, when transiently expressed in mammalian cells, we observed relatively low expression levels for all of the AKT Nbs. In a Co-IP experiment of AKT and the transiently expressed Nbs, we were only able to detect AKT for AKT3PH Nb8, which interacts with all three isoforms and had already shown to be an exceptional binder in a Co-IP using recombinant Nb. It is highly likely that the low expression levels of the Nbs lie at the base of the lack of signal for the other tested Nbs. Although this is in our experience exceptional, it is also possible that the correct folding of the Nbs is affected by the reducing cytoplasmic environment, resulting in a loss-of-function. Taking this into account together with the low Nb expression levels, these Nbs would benefit from alternative strategies to introduce the proteins into mammalian cells such as cell penetrating peptides, photoporation or electroporation(39).

Apart from interfering with AKT functions directly, an AKT isoform-specific Nb can be transformed into a tool to study protein function. Through the use of delocalization tags, a Nb can displace a target from its natural environment or when linked to a cullin-RING E3 ubiquitin ligase, the Nbs interaction with its target can trigger degradation of the target as an elegant alternative to RNAi(31, 40). A co-crystal structure of the Nb and its target can also be used for structure-based drug design and lead to the first true AKT isoform-specific inhibitor, this would be particularly interesting for AKT1PHE17K Nb7 and AKT2FL Nb8 as these Nbs have shown to interfere with the AKT PH-domain PIP3 interaction(41–43).

In this study, we generated and characterized AKT1 and AKT2 isoform-specific binders (Table 1) that can be made into research tools to study the isoform-specific functions of the AKT kinase. Additionally, two of these Nbs have shown to interfere with the AKT activation mechanism in an in vitro assay.

Table 1

Summary of characteristics for relevant AKT nanobodies.

Nanobody	Specificity (Co-IP)	Epitope (AKT domain)	Relative expression levels (MDA-MB-231)	Interferes with PH-PIP3 interaction
1PHE17K Nb7	AKT1	PH	Medium	Yes
2FL Nb5	AKT2	Linker/ catalytic	High	N/A
2FL Nb8		Regulatory	Medium	N/A
2FL Nb9		PH	Low	Yes
3PH Nb8	AKT1,2,3	PH	Low	No

The Co-IP of AKT using recombinant Nbs was used as final criterium for specificity. For the AKT2 set the Nbs' epitope was determined through ELISA, other Nb sets were generated by immunization with the PH-domain. Relative transient expression levels of the AKT Nbs in MDA-MB-231 cells was evaluated though Western blotting. AKT1PHE17K Nb7 and AKT2FL Nb2 interfere with the interaction the PH domain with PIP3 for the AKT1PH-, AKT1PHE17K- and AKT2PH-domain respectively. A summary of the characterization for the full Nb sets can be found in Additional file1: Table S1.

Conclusions

The high prevalence of AKT over-activation in cancer makes this kinase a high-profile target for cancer therapy. The currently available inhibitors do not discriminate between the three isoforms resulting in a zero sum when the isoforms have opposed functions – as is the case for AKT1 and AKT2 in breast cancer cells – or the toxicity observed in clinical trials. It is clear that new tools are needed to overcome these inhibitors' shortcomings. The Nbs obtained in this study are isoform-specific binders for AKT1 or AKT2. These can be made into research tools to investigate the isoform-specific functions of the AKT kinases in cells, offering alternatives to genetic approaches that will enable us to target a single AKT isoform. Additionally, two of these Nbs have shown to interfere with the AKT activation mechanism in an in vitro assay. These tools offer new opportunities to study the isoform-specific functions of AKT1 or AKT2 – and could lead to the first isoform-specific inhibitor.

Methods

Immunization, library construction and panning

AKT-PH domain production

Plasmids containing constructs coding for HA-AKT1, Myc-AKT1E17K, HA-AKT2 and HA-AKT3 were kind gifts from Donghwa Kim (H. Lee Moffit Cancer Center and Research Institute). cDNA encoding the PH-domains were isolated by PRC amplification using the following primers: Akt1PH Forward (Fwd) 5' AGC

GAA TTC ATG AGC GAC GTG GCT ATT GTG 3', Akt1PH Reverse (Rev) 5' GAA GCT TTC AGT TGT CAC TGG GTG AGC CCG ACC G 3, Akt2PH Fwd 5' AGC GAA TTC ATG AAT GAG GTG TCT GTC ATC 3', Akt2PH Rev 5' GAA GCT TTC ACA TCC ACT CCT CCC TCT CGT CTG G 3' Akt3PH Fwd 5' AGC GAA TTC ATG AGC GAT GTT ACC ATT GTG 3' and Akt3PH Rev 5' GAA GCT TTC AAT TCA TTC TCT CCT CTT CTT GCC TCT GC 3'. Constructs were inserted into a pHEN6 vector backbone using the Cold Fusion™ cloning kit (System Biosciences) according to the manufacturers' protocol and proteins were expressed in BL21 E. coli.

Immunization and panning

Nbs were generated in collaboration with the VIB Nanobody Service Facility as described in 'Generation of single domain antibody fragments derived from camelids and generation of manifold constructs' from Antibody Engineering: Methods and Protocols, second edition (2012). In short, alpacas were injected subcutaneously with the antigens on days 0, 7, 14, 21, and 35. Each injection contained 160 µg of protein for AKT1PH, 135 µg for AKT1PHE17K, 115 µg for AKT2FL and 250 µg for AKT3PH. Anticoagulated blood was collected on day 39. mRNA was extracted from lymphocytes, a VHH library was constructed and subjected to phage-display to select antigen-binding Nbs.

In Vitro Nanobody Characterization

Expression of recombinant AKT nanobodies

Heat Shock-competent WK6 E. coli (strain created by Dr. Gholamreza Hassanzadeh-Ghassabeh Nanobody Service Facility, VIB) were transformed with the AKT Nb constructs in a pMECS-(AKT2FL and AKT1PH) or pHEN4-vector backbone (AKT1PHE17K and AKT3PH) and grown overnight (ON) at 37 °C on a lysogeny broth (LB 10 g/L tryptone, 5 g/L yeast extract, 5 g/L NaCl)-agar plate containing 100 µg/mL Ampicillin. A single colony was picked and grown ON at 37 °C in a shaking incubator in LB with 100 µg/ml Ampicillin. The next day, 1/100 (v/v) was transferred to Terrific Broth (TB 16.9 mM KH_2PO_4, 71.9 mM $K_2HPO_4.3H_2O$, 2 mM $MgCl_2$, 12 g Tryptone, 24 g yeast extract, 4% glycerol, 1% glucose pH 7.2), grown to OD_{600} = 0.6–0.9, induced with 1 mM isopropylβ-D-thiogalactoside (IPTG) and incubated ON at 28 °C in a shaking incubator. The next day, cultures were centrifuged at 4 °C, 3,000 x g for 20 min. Nbs constructs in the pMECS- or pHEN4-vector are equipped with an N-terminal PelB signal sequence resulting in export of the Nbs to the periplasmatic space of E. coli and can be extracted through osmotic shock. Periplasmatic extracts were prepared by re-suspending the pellet in Tris-EDTA-sucrose buffer (TES) (0.2 M Tris-HCl, 0.5 mM EDTA and 0.5 M sucrose pH 8) and incubating for 1 h on ice with gentle agitation after which TES buffer diluted 4x in Milli-Q grade water was added and incubated for an additional hour (with shaking). Extracts were centrifuged at 4 °C, 29,000 x g for 20 min and the supernatant (SN) was collected.

ELISA

A 96-multiwell plate (Nunc Maxisorp, Sigma-Aldrich) was coated overnight (ON) at 4 °C with AKT1PH, AKT1PHE17K, AKT2PH or AKT3PH at 1 µg/mL in Coating buffer (100 mM $NaHCO_3$, pH 8.4). In between each of the subsequent steps, the plate was washed three times with 0.1% Tween in Phosphate Buffered

Saline (PBS) (-Ca^{2+}/Mg^{2+}). The remaining protein-binding sites were blocked by incubation with 0.1% (w/v) Casein in PBS for 1 h at room temperature (RT). Periplasmatic extract from WK6 E. coli containing a Nb was diluted in PBS (-Ca^{2+}/Mg^{2+}) and 100 µl was added to a well in quadruplicate for each for each PH-domain. After 1 h incubation at RT, each well was incubated (1 h at RT) with 100 µl 0.5 µg/mL anti-HA (#901502, BioLegend) antibody (Ab) and subsequently (1 h at RT) with 100 µl 0.5 µg/mL alkaline phosphatase (AP)-linked anti-mouse Ab (A90-116AP, Bethyl Laboratories). The reaction was initiated by adding 2 mg/mL AP substrate (4-nitrophenyl phosphate disodium salt hexahydrate, Sigma) in AP Blot Buffer (100 mM Tris-HCl, 50 mM $MgCl_2.6H_2O$, 100 mM NaCl, pH 9.50). Absorbance was measured at 405 nm. When the measured absorbance for an AKT Nb was at least threefold higher than for the EFGP Nb, the AKT Nb was considered to interact with that particular PH-domain. Significant differences in normalized OD_{405} were detected using a One-way ANOVA with Tukey's test using GraphPad Prism V5.00.

Co-immunoprecipitation endogenous AKT isoforms with recombinant nanobodies

Nbs were produced and extracted as described above. Anti-HA-agarose beads (A2095, Sigma Aldrich) were incubated with 10 µg periplasmatic extract for 1 h at 4 °C with end-over-end rotation. The beads were washed with ice-cold Tris Lysis Buffer (20 mM Tris-HCl, 150 mM NaCl, 1% Triton X-100 pH 7.5), 1 mM phenyl-metylsulfonyl fluoride (PMSF) and 200 µg/mL protease inhibitor cocktail) and incubated for 1 h at 4 °C with end-over-end rotation with 1 mg crude lysate from MDA-MB-231 cells. A negative control where no Nb was added to the beads was included to determine non-specific binding of AKT to the agarose matrix. The beads were washed three times with excess Tris Lysis buffer and heated to 95 °C for 5 min in Laemmli Sample Buffer (5% SDS, 20% glycerol, 0,2% bromophenol blue, 5% β-mercaptoethanol, 65 mM Tris-HCl pH 6.8). Samples were analyzed by SDS-PAGE and Western blotting. The AKT isoforms were detected using isoform-specific Abs (AKT1 C73H10, AKT2 D6G4 and AKT3 62A8 from Cell Signaling Technology®) and the Nbs with an anti-HA-tag Ab (11583816001, Merck).

Epitope mapping of AKT2FL nanobodies

Nanobodies were produced as described in "Expression of recombinant AKT nanobodies". The AKT2 PH domain was produced as described above, the other AKT2 fragments were created through PCR amplification based on the HA-AKT2 template using the following primers: FL-AKT2 Fwd: 5' TGT ACA GAA TGC TGG TCA TAT GAA TGA GGT GTC TGT CAT C 3' and FL-AKT2 Rev: 5' TCA CCC GGG CTC GAG GAA TTC TCA CTC GCG GAT GCT GGC CGA GTA GG 3' for full-length AKT2, AKT2AA111 Fwd: 5' TGT ACA GAA TGC TGG TCA TAT GAA GCA GCG GGC CCC AGG CG 3' and FL-AKT2 Rev for AKT2AA111 and AKT2Reg Fwd: 5' GTA CAG AAT GCT GGT CAT ATG CTC AGC ATC AAC TGG CAG 3' and FL-AKT2 Rev for the AKT2 Regulatory domain. PCR product was cloned into the pTYB12 vector using the Cold Fusion™ cloning kit (System Biosciences) according to the manufacturers' protocol. BL21 E. coli were heat-shock transformed with the AKT2 constructs in a pTYB12 vector backbone. A culture was grown in TB to an OD_{600} > 2, expression of the constructs induced with 0.5 mM IPTG and the culture was incubated ON at 20 °C in a shaking incubator. The following day, the cultures were centrifuged (20 min at 3000 x g, 4 °C) and re-suspended in Chitin column buffer (20 mM Tris-HCl, 500 mM NaCl and 1 mM EDTA, pH 8.5) with

1 mM PMSF and 200 µg/mL protease inhibitor cocktail. Cells were lysed using a French Press and sonication. Debris was pelleted by centrifugation (20 min at 29,000 x g, 4 °C), supernatant was collected and loaded onto a column with Chitin beads (New England Biolabs) and allowed to empty by gravity flow at approximately 1 ml/min. Beads were washed with column buffer and incubated ON with column buffer containing 50 mM dithiothreitol (DTT). Elutions were collected and analysed by SDS-PAGE and Coomassie staining. The ELISA epitope mapping was performed as described above with the AKT2 constructs coated in the wells and AKT2FL Nbs (in crude periplasmatic extract) added in solution.

PIP3 pull-down

Nbs from a periplasmatic extract were purified using TALON™-IMAC (Clontech) according to the manufacturers' protocol. In short, periplasmatic extracts were incubated for 2 h at 4 °C with end-over-end rotation with TALON™ resin pre-equilibrated with wash buffer (50 mM NaH_2PO_4, 500 mM NaCl and 20 mM imidazole, pH 8). The resin was washed three times with wash buffer and bound proteins were eluted with elution buffer (50 mM NaH_2PO_4, 500 mM NaCl and 500 mM imidazole, pH 8). Purity of the proteins was evaluated using SDS-PAGE and Coomassie staining.

For the pull-down experiment, a Nb was incubated at a 10X molar excess with PH-domain in Binding Buffer (10 mM HEPES, 150 mM NaCl and 0.25% NP-40, pH 7.4) for 1 h at 4 °C with end-over end rotation. Subsequently 50 µl PIP3-coated beads (P-B345A, Echelon Biosciences) were added to the mixture. A negative control containing only beads and a PH-domain was also included at this point. After a 3 h incubation at 4 °C with end-over-end rotation, the beads were washed three times with Binding Buffer and bound proteins were eluted by adding Laemmli sample buffer and heating the beads to 95 °C for 5 min. Proteins were separated by size through SDS-PAGE followed by Western Blot analysis. AKT1 and AKT2 were detected using an isoform-specific Ab (AKT1 C73H10 and AKT2 D6G4, Cell Signaling Technology®) and AKT3 using an anti-His_6-tag Ab (631212, Clontech).

In vivo AKT Nanobody properties

Subcloning Nbs for expression in mammalian cells

Nbs were subcloned to the pcDNA3.1 V5/His_6 vector for transient expression in mammalian cells. PCR amplification of the Nbs was performed using 5′TTG GTA CCG AGC TCG GCC ACC ATGCAG GTG CAG CTG CAG GAG 3′ and 5′TAG ACT CGA GCG GCC GCT GGA GAC GGT GAC CTG 3′ as forward and reverse primer respectively. Cloning was performed with the Cold Fusion™ cloning kit (System Biosciences) according to the manufacturers' protocol.

Cell Culture, transfection & pull-down

MDA-MB-231 (ATCC® HTB-26™) cells were cultured in Dulbecco's Modified Eagle Medium (DMEM, Gibco, Thermo Fisher Scientific) supplemented with 10% fetal bovine serum (Gibco, Thermo Fisher Scientific), 100 IU/mL penicillin and 10 µg/mL streptomycin (Gibco, Thermo Fisher Scientific). Cells were grown in a

humidified incubator at 37 °C and 10% CO_2. For transient expression of the AKT Nbs, the JetPrime® transfection reagent (Polyplus Transfection) was used according to the manufacturers' recommendations. 24 h after transfection, the cells were collected using Trypsin Ethylenediaminetetraacetic acid (EDTA, 0.05%, Gibco, Thermo Fisher Scientific) and lysed in ice-cold Tris Lysis Buffer. 1 mg crude extract was incubated with 10 µl settled anti-V5-agarose beads (A7345, Sigma Aldrich) for 1 h at 4 °C with end-over-end rotation. The beads were washed three times with Tris Lysis Buffer and bound proteins were eluted by adding Laemmli sample buffer and heating the samples to 95 °C for 5 min. Proteins were separated using SDS-PAGE and analyzed by Western Blotting. AKT was detected using a pan-AKT Ab (C67E7, Cell Signaling Technology) and the Nbs through their V5-tag with an anti-V5 Ab (R960-25, Thermo Fisher Scientific).

Abbreviations

PI3K
Phosphoinositide 3-kinase
AKT
Protein Kinase B
mTOR
mammalian target of ramapycin
PTEN
phosphatase and tensin homolog
PHLPP
PH domain and Leucine rich repeat Protein Phosphatase
PH
Pleckstrin homology
PIP3
phosphatidylinositol (3,4,5)-trisphosphate
HCAb
Heavy-Chain-Only antibody
IgG
immunoglobulin G
LC
Light-chain of an IgG
HC
Heavy chain of an IgG
VHH
variable domain of the heavy chain of a HCAb
Nb
Nanobody
FR

Framework Region
HV
Hypervariable Region
CDR
complementarity-determining region
VH
variable domain of the Heavy chain
VL
variable domain of the Light chain
AKT1PH
Recombinant PH domain of the AKT1 isoform
AKT1PHE17K
Recombinant PH domain of the AKT1 isoform where the 17th amino acid residue (Glutamic Acid) is mutated to Lysine
AKT2FL
Full-length AKT2 isoform produced in SF9 cells and in vitro phosphorylated on T308 and S474
AKT3PH
recombinant PH domain of the AKT3 isoform
IMAC
immobilized metal affinity chromatography
ELISA
enzyme-linked immunosorbent assay
OD
optical density
CI
confidence interval
Co-IP
Co-immunoprecipitation
HA
hemagluttin
FL-AKT2
recombinant full-length AKT2 produced in E. coli
AKT2AA111
recombinant AKT2 lacking the PH domain
AKT2REG
recombinant AKT2 C-terminal regulatory domain
PCR
polymerase chain reaction
Fwd
Forward primer

Rev
Reverse primer
ON
Overnight
LB
Lysongeny Broth
TB
Terrific broth
IPTG
isopropyl β-D-thiogalactoside
TES
tris-EDTA-sucrose buffer
SN
supernatant
PBS
Phosphate Buffered saline
RT
Room temperature; Ab:antibody
AP
alkaline phosphatase
PMSF
phenyl-metylsulfonyl fluoride
DTT
dithiothreitol
DMEM
Dulbecco's Modified Eagle Medium
EDTA
Ethylenediaminetetraacetic acid

Declarations

Competing interests
Declaration of financial competing interest: J.G. is shareholder of Gulliver Biomed BV. J.G. declares that he has no non-financial competing interests. T.M., O.Z. and K.G. declare no potential conflicts of interest.
Funding
T.M. is supported by Fonds Wetenschappelijk Onderzoek (1S 127 16N) and Ghent University (30322401).
Author's contributions
T.M. and J.G. were responsible for the study design. T.M. and O.Z. performed all experiments. T.M., J.G. and K.G. wrote the manuscript. All authors reviewed the manuscript.
Acknowledgements

The authors thank Dr. Gholamreza Hassanzadeh-Ghassabeh (Nanobody Core, Vlaams Instituut voor Biotechnologie (VIB), Brussels, Belgium) for the identification of AKT nanobodies by phage panning. Plasmids containing constructs coding for HA-AKT1, Myc-AKT1E17K, HA-AKT2 and HA-AKT3 were kind gifts from Donghwa Kim (H. Lee Moffit Cancer Center and Research Institute).

Authors information (optional)

Not applicable

Availability of data and materials

All experimental data generated or analysed during this study are included in this published article and its supplementary information files. AKT nanobody cDNA sequences are under licence from Gulliver Biomed BV and are not publicly available.

References

1.
Shaw RJ, Cantley LC. Ras. PI(3)K and mTOR signalling controls tumour cell growth. Nature. 2006;441(7092):424–30.
2.
Mayer IA, Arteaga CL. The PI3K/AKT Pathway as a Target for Cancer Treatment. In: Caskey CT, editor. Annual Review of Medicine, Vol 67. Annual Review of Medicine. 67. Palo Alto: Annual Reviews; 2016. p. 11–28.
3.
Toker A, Yoeli-Lerner M. Akt signaling and cancer: Surviving but not moving on. Cancer Res. 2006;66(8):3963–6.
4.
Song MQ, Bode AM, Dong ZG, Lee MH. AKT as a Therapeutic Target for Cancer. Cancer Res. 2019;79(6):1019–31.
5.
Wu WI, Voegtli WC, Sturgis HL, Dizon FP, Vigers GPA, Brandhuber BJ. Crystal Structure of Human AKT1 with an Allosteric Inhibitor Reveals a New Mode of Kinase Inhibition. PLoS One. 2010;5(9):9.
6.
Yang J, Cron P, Good VM, Thompson V, Hemmings BA, Barford D. Crystal structure of an activated Akt/protein kinase B ternary complex with GSK3-peptide and AMP-PNP. Nat Struct Biol. 2002;9(12):940–4.
7.
Nitulescu GM, Margina D, Juzenas P, Peng Q, Olaru OT, Saloustros E, et al. Akt inhibitors in cancer treatment: The long journey from drug discovery to clinical use. Int J Oncol. 2016;48(3):869–85.
8.
Okuzumi T, Fiedler D, Zhang C, Gray DC, Aizenstein B, Hoffman R, et al. Inhibitor hijacking of Akt activation. Nat Chem Biol. 2009;5(7):484–93.
9.

Sangai T, Akcakanat A, Chen HQ, Tarco E, Wu Y, Do KA, et al. Biomarkers of Response to Akt Inhibitor MK-2206 in Breast Cancer. Clin Cancer Res. 2012;18(20):5816–28.
10.
Uhlenbrock N, Smith S, Weisner J, Landel I, Lindemann M, Le TA, et al. Structural and chemical insights into the covalent-allosteric inhibition of the protein kinase Akt. Chem Sci. 2019;10(12):3573–85.
11.
Wang J, Zhao W, Guo HF, Fang Y, Stockman SE, Bai S, et al. AKT isoform-specific expression and activation across cancer lineages. BMC Cancer. 2018;18:10.
12.
Clark AR, Toker A. Signalling specificity in the Akt pathway in breast cancer. Biochem Soc Trans. 2014;42:1349–55.
13.
Parikh C, Janakiraman V, Wu WI, Foo CK, Kljavin NM, Chaudhuri S, et al. Disruption of PH-kinase domain interactions leads to oncogenic activation of AKT in human cancers. Proc Natl Acad Sci U S A. 2012;109(47):19368–73.
14.
Calleja V, Alcor D, Laguerre M, Park J, Vojnovic B, Hemmings BA, et al. Intramolecular and intermolecular interactions of protein kinase B define its activation in vivo. PLoS Biol. 2007;5(4):780–91.
15.
Calleja V, Laguerre M, Parker PJ, Larijani B. Role of a Novel PH-Kinase Domain Interface in PKB/Akt Regulation: Structural Mechanism for Allosteric Inhibition. PLoS Biol. 2009;7(1):189–200.
16.
Riggio M, Perrone MC, Polo ML, Rodriguez MJ, May M, Abba M, et al. AKT1 and AKT2 isoforms play distinct roles during breast cancer progression through the regulation of specific downstream proteins. Sci Rep. 2017;7:12.
17.
Peres J, Mowla S, Prince S. The T-box transcription factor, TBX3, is a key substrate of AKT3 in melanomagenesis. Oncotarget. 2015;6(3):1821–33.
18.
Cariaga-Martinez AE, Lopez-Ruiz P, Nombela-Blanco MP, Motino O, Gonzalez-Corpas A, Rodriguez-Ubreva J, et al. Distinct and specific roles of AKT1 and AKT2 in androgen-sensitive and androgen-independent prostate cancer cells. Cell Signal. 2013;25(7):1586–97.
19.
Santi SA, Lee H. Ablation of Akt2 Induces Autophagy through Cell Cycle Arrest, the Downregulation of p70S6K, and the Deregulation of Mitochondria in MDA-MB231 Cells. PLoS One. 2011;6(1):15.
20.
Chin YR, Toker A. Akt isoform-specific signaling in breast cancer Uncovering an anti-migratory role of palladin. Celll Adhes Migr. 2011;5(3):211–4.
21.

Dillon RL, Marcotte R, Hennessy BT, Woodgett JR, Mills GB, Muller WJ. Akt1 and Akt2 Play Distinct Roles in the Initiation and Metastatic Phases of Mammary Tumor Progression. Cancer Res. 2009;69(12):5057–64.
22.
Brognard J, Sierecki E, Gao TY, Newton AC. PHLPP and a second isoform, PHLPP2, differentially attenuate the amplitude of Akt signaling by regulating distinct Akt isoforms. Mol Cell. 2007;25(6):917–31.
23.
Maroulakou IG, Oemler W, Naber SP, Tsichlis PN. Akt1 ablation inhibits, whereas Akt2 ablation accelerates, the development of mammary adenocarcinomas in mouse mammary tumor virus (MMTV)-ErbB2/Neu and MMTV-polyoma middle T transgenic mice. Cancer Res. 2007;67(1):167–77.
24.
Arboleda MJ, Lyons JF, Kabbinavar FF, Bray MR, Snow BE, Ayala R, et al. Overexpression of AKT2/protein kinase B beta leads to up-regulation of beta 1 integrins, increased invasion, and metastasis of human breast and ovarian cancer cells. Cancer Res. 2003;63(1):196–206.
25.
Chin YR, Toker A. The Actin-Bundling Protein Palladin Is an Akt1-Specific Substrate that Regulates Breast Cancer Cell Migration. Mol Cell. 2010;38(3):333–44.
26.
Irie HY, Pearline RV, Grueneberg D, Hsia M, Ravichandran P, Kothari N, et al. Distinct roles of Akt1 and Akt2 in regulating cell migration and epithelial-mesenchymal transition. J Cell Biol. 2005;171(6):1023–34.
27.
Wang Q, Chen XY, Hay N. Akt as a target for cancer therapy: more is not always better (lessons from studies in mice). Br J Cancer. 2017;117(2):159–63.
28.
Hamerscasterman C, Atarhouch T, Muyldermans S, Robinson G, Hamers C, Songa EB, et al. NATURALLY-OCCURRING ANTIBODIES DEVOID OF LIGHT-CHAINS. Nature. 1993;363(6428):446–8.
29.
Muyldermans S, Baral TN, Retarnozzo VC, De Baetselier P, De Genst E, Kinne J, et al. Camelid immunoglobulins and nanobody technology. Vet Immunol Immunopathol. 2009;128(1–3):178–83.
30.
Muyldermans S. Nanobodies: Natural Single-Domain Antibodies. In: Kornberg RD, editor. Annual Review of Biochemistry, Vol 82. Annual Review of Biochemistry. 82. Palo Alto: Annual Reviews; 2013. p. 775 – 97.
31.
Beghein E, Gettemans J. Nanobody Technology: A versatile Toolkit for Microscopic imaging, Protein-Protein interaction Analysis, and Protein Function exploration. Front Immunol. 2017;8:14.
32.
Decanniere K, Muyldermans S, Wyns L. Canonical antigen-binding loop structures in immunoglobulins: More structures, more canonical classes? J Mol Biol. 2000;300(1):83–91.
33.

De Genst E, Silence K, Decanniere K, Conrath K, Loris R, Kinne R, et al. Molecular basis for the preferential cleft recognition by dromedary heavy-chain antibodies. Proc Natl Acad Sci U S A. 2006;103(12):4586–91.
34.
Bertier L, Hebbrecht T, Mettepenningen E, De Wit N, Zwaenepoel O, Verhelle A, et al. Nanobodies targeting cortactin proline rich, helical and actin binding regions downregulate invadopodium formation and matrix degradation in SCC-61 cancer cells. Biomed Pharmacother. 2018;102:230–41.
35.
Molife LR, Yan L, Vitfell-Rasmussen J, Zernhelt AM, Sullivan DM, Cassier PA, et al. Phase 1 trial of the oral AKT inhibitor MK-2206 plus carboplatin/paclitaxel, docetaxel, or erlotinib in patients with advanced solid tumors. J Hematol Oncol. 2014;7:12.
36.
Carpten JD, Faber AL, Horn C, Donoho GP, Briggs SL, Robbins CM, et al. A transforming mutation in the pleckstrin homology domain of AKT1 in cancer. Nature. 2007;448(7152):439-U1.
37.
Beaver JA, Gustin JP, Yi KH, Rajpurohit A, Thomas M, Gilbert SF, et al. PIK3CA and AKT1 Mutations Have Distinct Effects on Sensitivity to Targeted Pathway Inhibitors in an Isogenic Luminal Breast Cancer Model System. Clin Cancer Res. 2013;19(19):5413–22.
38.
Kumar A, Purohit R. Cancer Associated E17K Mutation Causes Rapid Conformational Drift in AKT1 Pleckstrin Homology (PH) Domain. PLoS One. 2013;8(5):10.
39.
Liu J, Hebbrecht T, Brans T, Parthoens E, Lippens S, Li CN, et al. Long-term live-cell microscopy with labeled nanobodies delivered by laser-induced photoporation. Nano Res.11.
40.
Fulcher LJ, Hutchinson LD, Macartney TJ, Turnbull C, Sapkota GP. Targeting endogenous proteins for degradation through the affinity-directed protein missile system. Open Biol. 2017;7(5):11.
41.
Lawson ADG. Antibody-enabled small-molecule drug discovery. Nat Rev Drug Discov. 2012;11(7):519–25.
42.
Quevedo CE, Cruz-Migoni A, Bery N, Miller A, Tanaka T, Petch D, et al. Small molecule inhibitors of RAS-effector protein interactions derived using an intracellular antibody fragment. Nat Commun. 2018;9:12.
43.
Vasylieva N, Kitamura S, Dong JX, Barnych B, Hvorecny KL, Madden DR, et al. Nanobody-based binding assay for the discovery of potent inhibitors of CFTR inhibitory factor (Cif). Anal Chim Acta. 2019;1057:106–13.

Figures

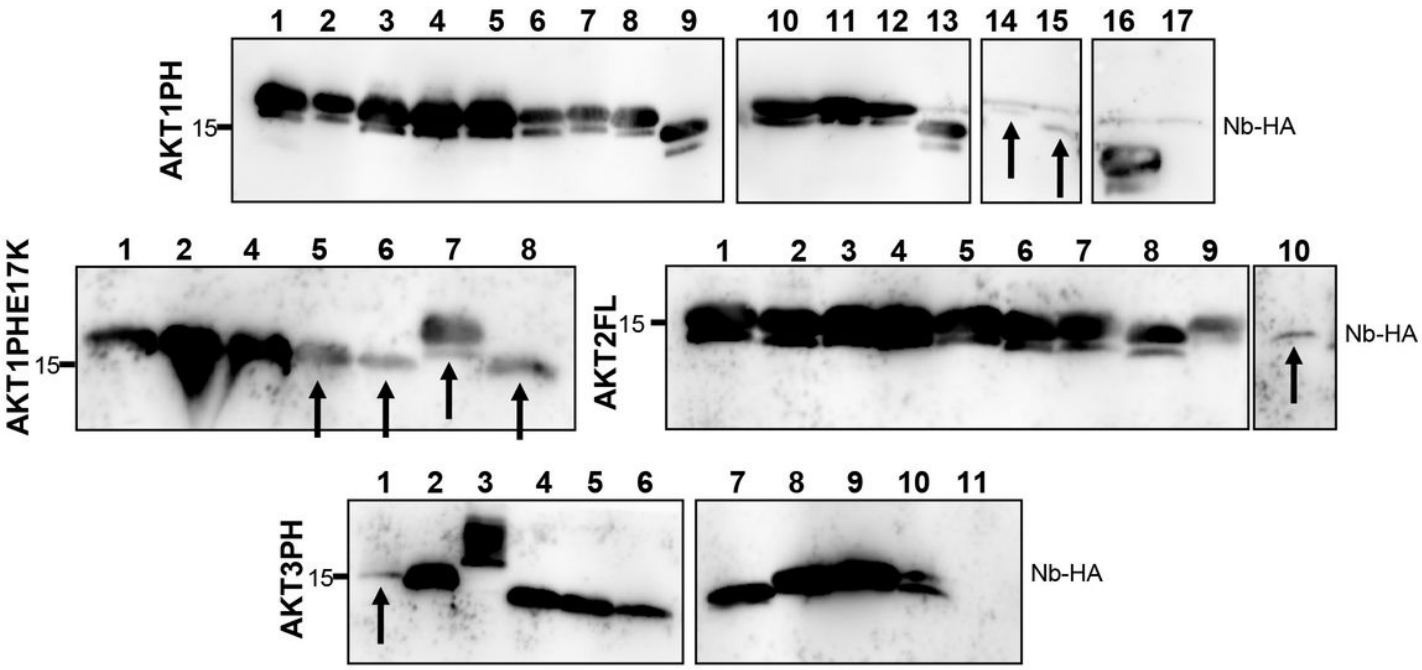

Figure 1

Expression of AKT nanobodies in WK6 E. coli. Western blot detection of AKT Nbs in a crude periplasmatic extract on a 15% SDS gel. An anti-HA Ab was used to detect the Nbs. The vast majority of the Nbs have comparable and high expression yields. The expression of AKT1PH Nb14 and Nb15, AKT1PHE17K Nbs5-8, AKT2FL Nb10 and AKT3PH Nb1 is low (denoted by an arrow) whereas only AKT1PH Nb17 and AKT3PH Nb11 could not be detected. Uncropped blots are available in Additional file 1: Figure S2.

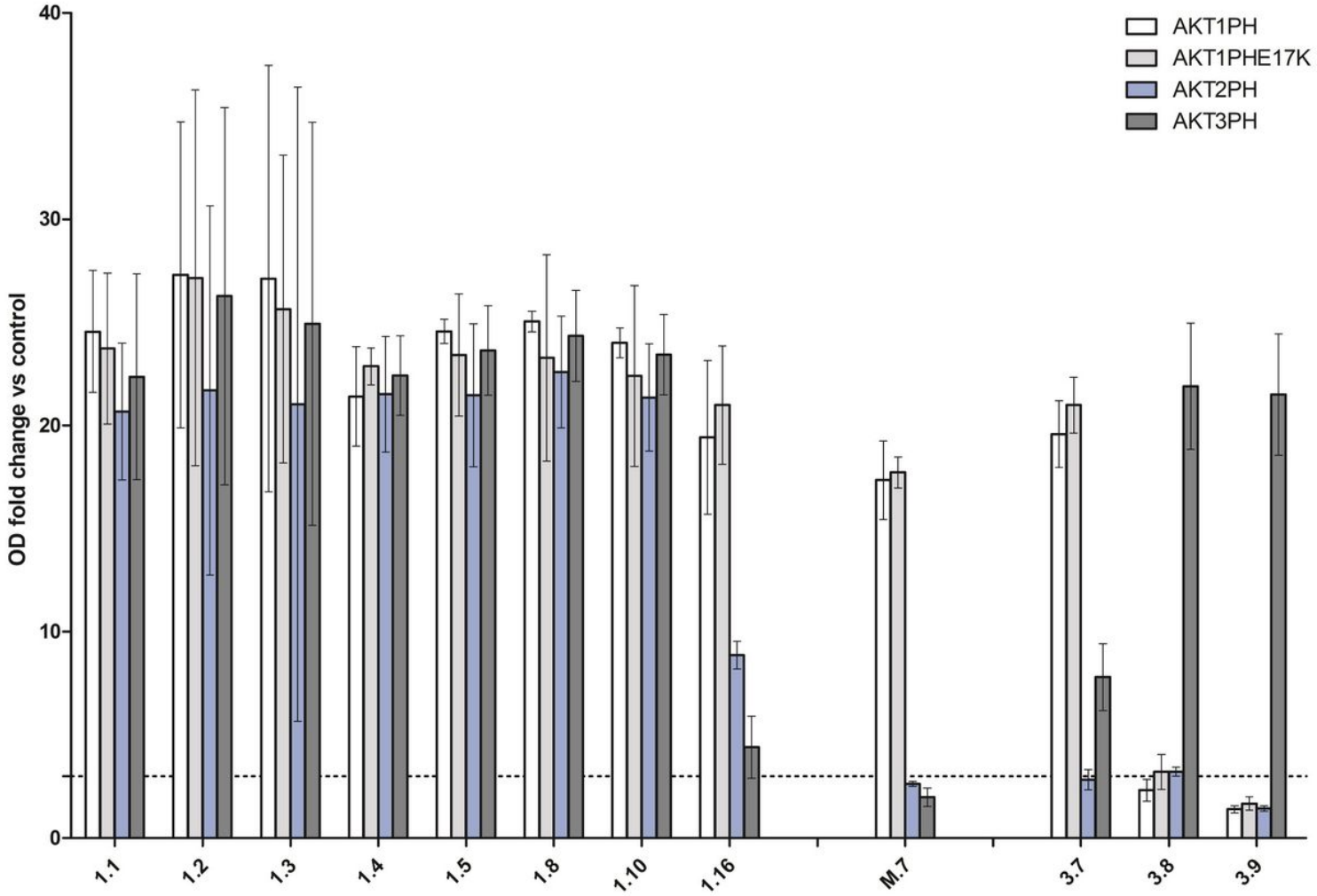

Figure 2

ELISA screening of AKT pleckstrin homology domain nanobodies. The mean and 95% confidence interval (CI) of normalized OD405 values are shown. Pleckstrin Homology domains were coated in 96 multiwell plates at 1µg/ml and incubated with the AKT Nbs (20µl from a crude periplasmatic extract). The EGFPNb is used for background correction. A Nb is considered to interact with a PH domain when the OD405 fold change (normalized to the OD405 of the EGFPNb for the same PH domain) is at least three (denoted by a dashed line). Nbs, which did not meet this criterion for any PH domain are not shown on this figure and were not included in further analysis. ELISA data for the complete Nb sets are available in Additional file 1: Figure S3.

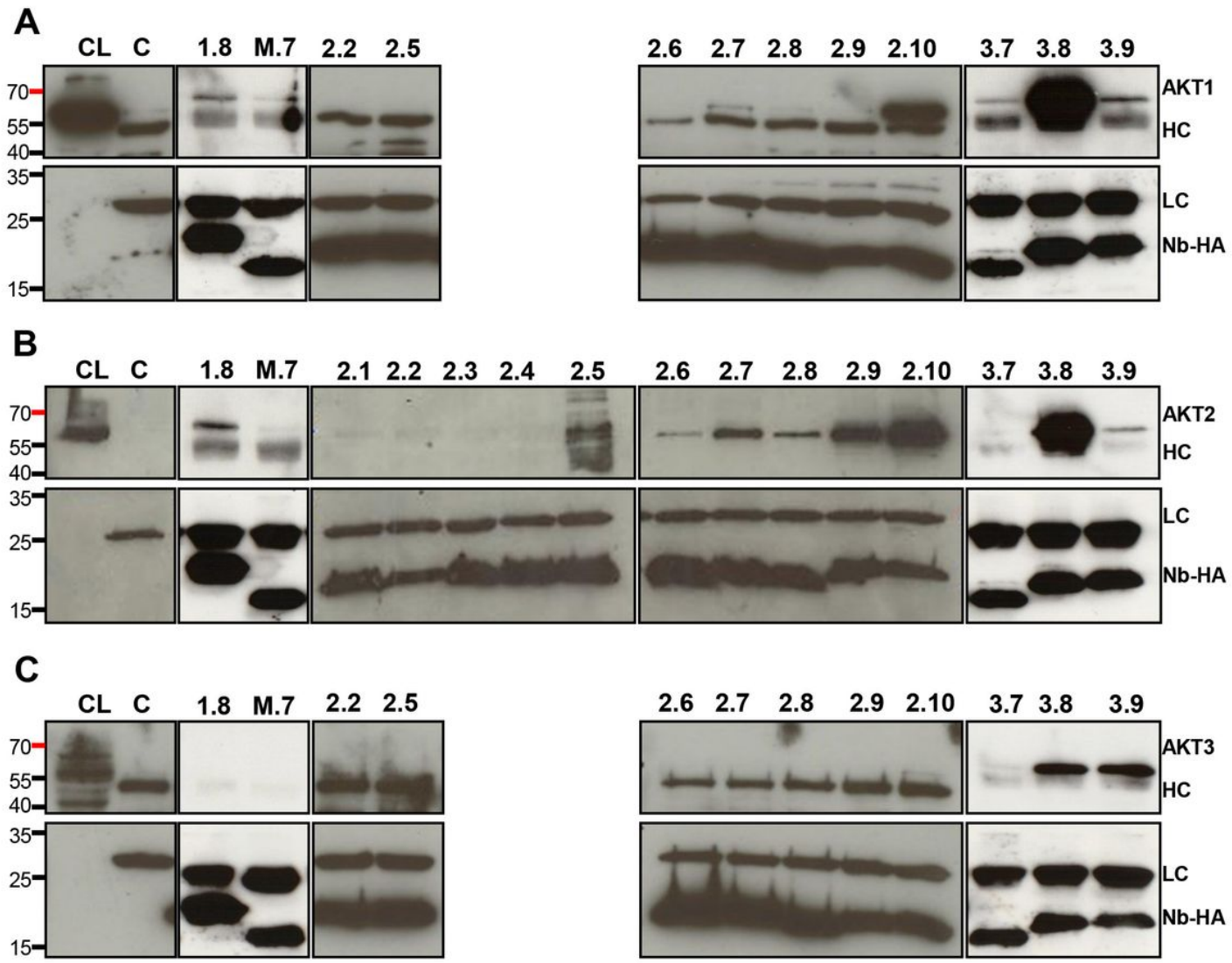

Figure 3

Co-IP of AKT isoforms using AKT1PH-, AKT1PHE17K-, AKT2FL- and AKT3PH-Nbs. Immunoprecipitation of endogenous AKT1 (A), AKT2 (B) or AKT3 (C) from MDA-MB-231 cells with recombinantly produced HA-tagged Nbs. CL= crude lysate, C= negative control of anti-HA-agarose and MDA-MB-231 lysate, HC= Heavy-Chain and LC= Light-Chain. The number above the lanes corresponds to the Nb that was used in that Co-IP i.e. 1.8 denotes Nb8 from the AKT1PH Nb set, M.7 is Nb7 from the AKT1PHE17K Nb set, 2.2 is Nb2 from the AKT2FL Nb set and 3.7 is Nb7 from the AKT3PH Nb set. Nbs were blotted using an anti-HA antibody, AKT1, AKT2 and AKT3 were detected using C73H10, D6G4 and 62A8 respectively. All nanobodies (Nb-HA) are efficiently expressed in E. coli. Uncropped blots are available in Additional file 1: Figure S4.

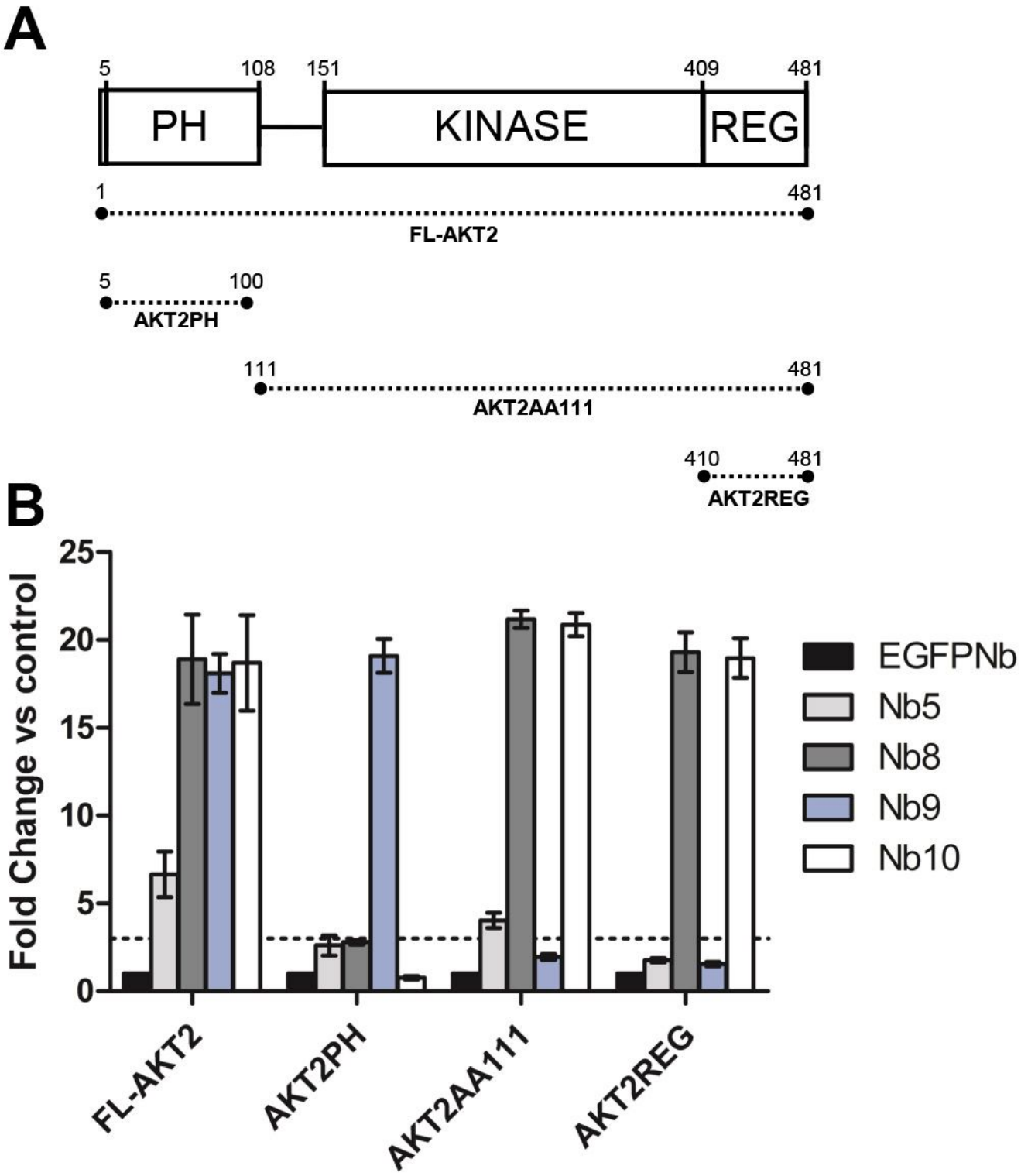

Figure 4

Epitope mapping of AKT2FL Nbs. A: Illustration of the AKT fragments used for epitope mapping. B: ELISA: Mean and 95% CI of normalized OD plotted for full-length AKT2 (FL-AKT2), the AKT2 PH domain (AKT2PH), a fragment consisting of the flexible linker, kinase domain and regulatory domain (AKT2AA111) and the regulatory domain (AKT2REG). Target proteins were coated in wells of a 96 multiwell plate in quadruplicate for each AKT2 Nb and the EGFP Nb (negative control). All measured OD's

were normalized for the negative control. A Nb was considered to be an interactor when the average normalized OD was at least three times that of the negative control for the same AKT2 fragment (dashed line).

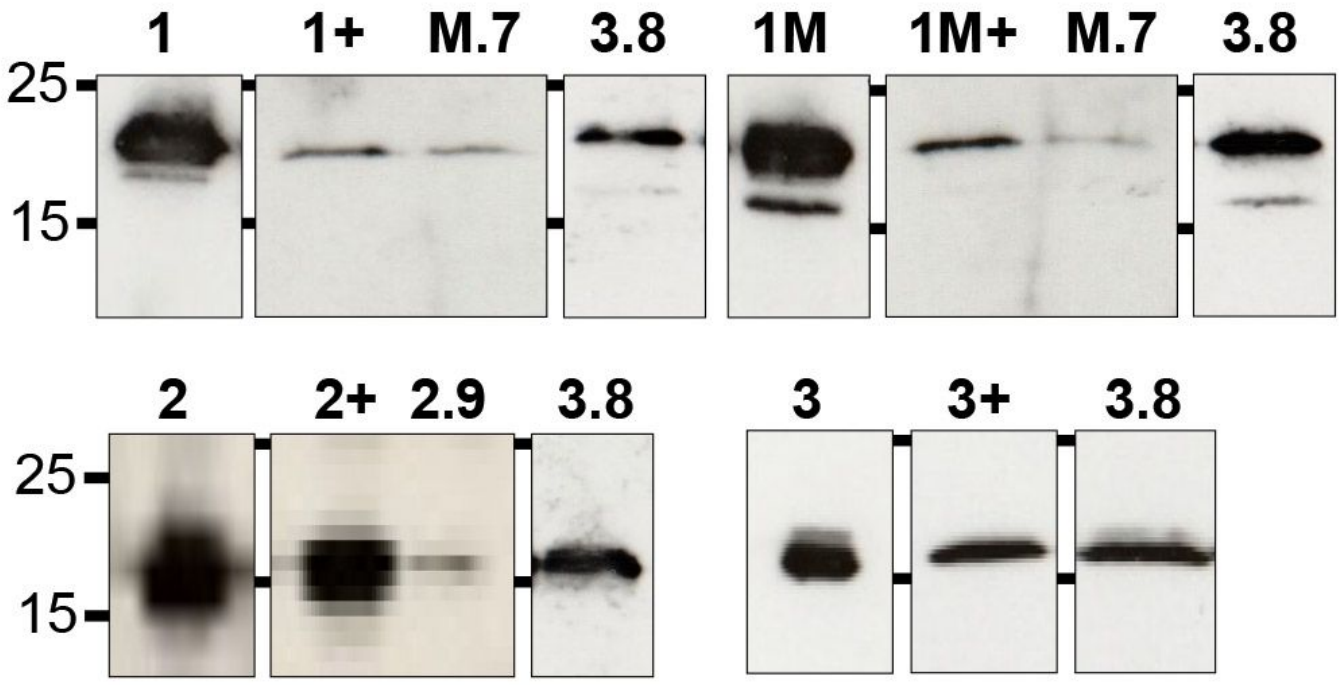

Figure 5

AKT Nanobodies interfere with AKT-PH—PIP3 interaction. Western Blot of pull-down experiments using PIP3—coated beads and the AKT PH-domains. 1= AKT1PH-, 1M= AKT1PHE17K-, 2= AKT2PH- and 3=AKT3PH-domain. For each PH domain a positive control was included where no Nb was added (1+, 1M+, 2+ and 3+ for the AKT1PH-, AKT1PHE17K– , AKT2PH– and AKT3PH-domain respectively). When the PH-domains are incubated with AKT1PHE17K Nb7 (M.7) or AKT2FL Nb9 (2.9) before PIP3-coated beads are added we observe a reduction in the signal for AKT1PH- and AKT1PHE17K- or AKT2PH-domain respectively. AKT3PH Nb8 (3.8) had no effect on the interaction of the PH-domains with the PIP3—coated beads. The AKT1PH– and AKT2PH-domain were detected using an Ab specific for AKT1 (C73H10) and AKT2 (D6G4) respectively the AKT3PH-domain was detected using an anti-His6-tag Ab. Uncropped blots are available in Additional file 1: Figure S5.

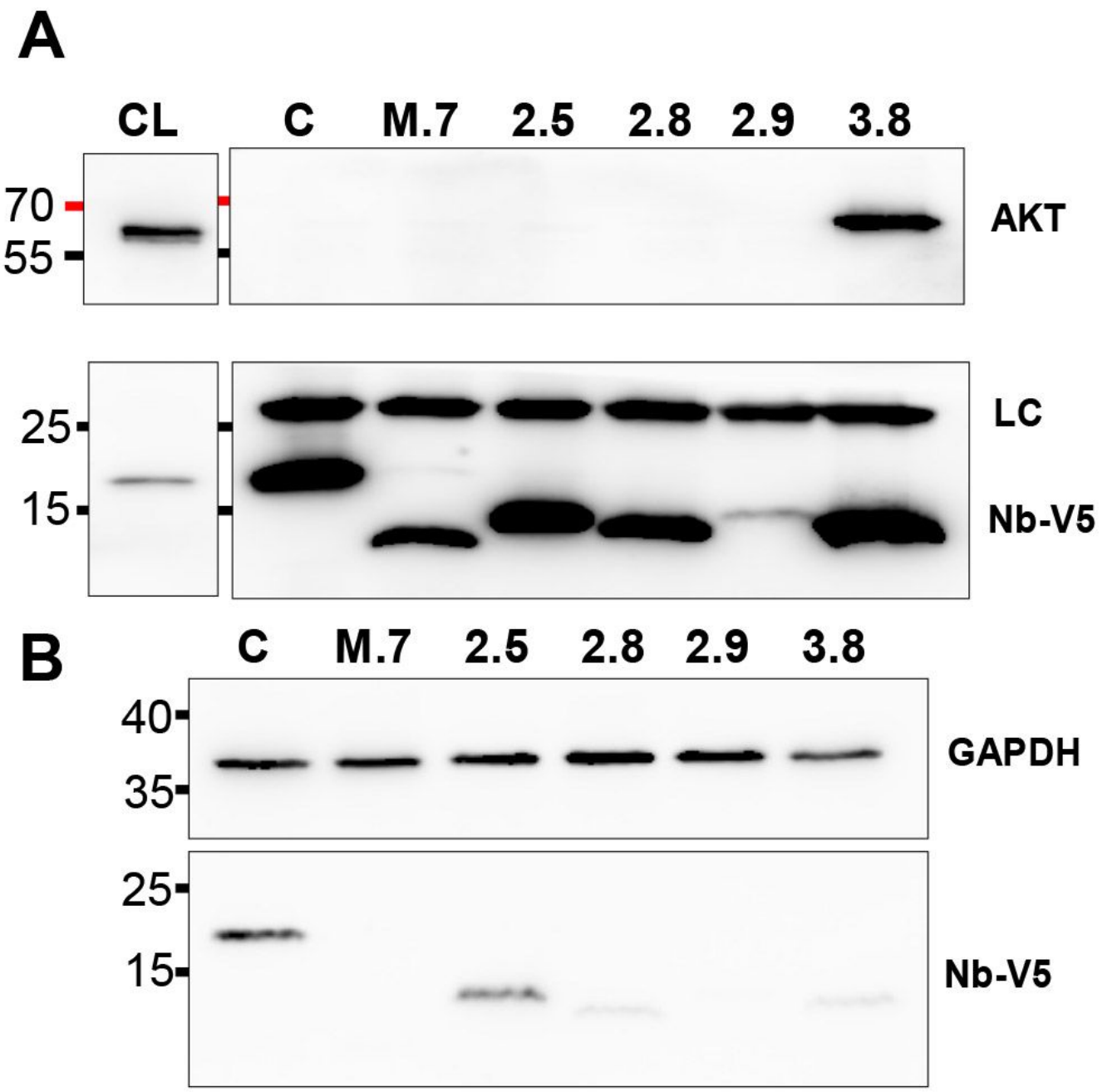

Figure 6

Co-IP of endogenous AKT from MDA-MB-231 cells with Nbs transiently expressed as intrabodies. A: Co-IP of AKT and Nbs. CL= crude lysate from EGFP Nb transfected cells, C= negative control with transient expression of the EGFP Nb. LC= Light Chain. B: Nb expression in crude lysate. 10µg crude lysate from transfected cells analysed through SDS-PAGE and western blotting. GAPDH signal was used as loading control. AKT was detected using a pan-AKT antibody (C67E7), Nbs were detected using an anti-V5-antibody. Uncropped blots are available in supplementary (Figure S6).

Supplementary Files

This is a list of supplementary files associated with this preprint. Click to download.

- Additionalfile1.pdf